European Journal of Pharmaceutics and Biopharmaceutics 85 (2013) 1006–1018

Contents lists available at SciVerse ScienceDirect

European Journal of Pharmaceutics and Biopharmaceutics

journal homepage: www.elsevier.com/locate/ejpb

Research paper

Particle sizing measurements in pharmaceutical applications: Comparison of in-process methods versus off-line methods

Ana F.T. Silva [a,f], Anneleen Burggraeve [a], Quenten Denon [b], Paul Van der Meeren [b], Niklas Sandler [c], Tom Van Den Kerkhof [d], Mario Hellings [d], Chris Vervaet [e], Jean Paul Remon [e], João Almeida Lopes [f], Thomas De Beer [a,*]

[a] Laboratory of Pharmaceutical Process Analytical Technology, Ghent University, Ghent, Belgium
[b] Particle and Interfacial Technology Group, Ghent University, Ghent, Belgium
[c] Pharmaceutical Sciences Laboratory,Department of Biosciences, Åbo Akademi University, Turku, Finland
[d] Johnson and Johnson Pharmaceutical Research and Development, Analytical Development, Beerse, Belgium
[e] Laboratory of Pharmaceutical Technology, Ghent University, Gent, Belgium
[f] REQUIMTE, Department of Chemical Sciences, University of Porto, Porto, Portugal

ARTICLE INFO

Article history:
Received 5 February 2013
Accepted in revised form 28 March 2013
Available online 10 April 2013

Keywords:
Particle size
PAT
In-process
Inline
FBRM
Spatial Filtering Velocimetry
Photometric Stereo Imaging
Eyecon®
Laser diffraction

ABSTRACT

It has been previously described that when a sample's particle size is determined using different sizing techniques, the results can differ considerably. The purpose of this study was to review several in-process techniques for particle size determination (Spatial Filtering Velocimetry, Focused Beam Reflectance Measurements, Photometric Stereo Imaging, and the Eyecon® technology) and compare them to well-known and widespread off-line reference methods (laser diffraction and sieve analysis). To start with, a theoretical explanation of the working mechanism behind each sizing technique is presented, and a comparison between them is established. Secondly, six batches of granules and pellets (i.e., spherical particles) having different sizes were measured using these techniques. The obtained size distributions and related D_{10}, D_{50}, and D_{90} values were compared using the laser diffraction wet dispersion method as reference technique. As expected, each technique provided different size distributions with different D values. These dissimilarities were examined and explained considering the measurement principles behind each sizing technique. The particle property measured by each particle size analyzer (particle size or chord length) and how it is measured as well as the way in which size information is derived and calculated from this measured property and how results are presented (e.g., volume or mass distributions) are essential for the interpretation of the particle size data.

1. Introduction

Building quality into pharmaceutical products is the leading purpose of the Process Analytical Technology (PAT) initiative [1]. Particle size is a critical quality parameter in a number of pharmaceutical unit operations such as pre-mixing/mixing, granulation, drying, milling, roller compaction, spray-drying, coating, and compression. An adequate particle size distribution (PSD) is essential to ensure optimal manufacturability which will have an important impact on the end product's safety, efficacy, and quality. Therefore, monitoring and controlling particle size via in-process particle size measurements is essential to the pharmaceutical industry.

The application of in-process particle sizing tools for the assessment of the influence of process and formulation parameters upon critical product quality attributes has been studied for several pharmaceutical processes such as fluid bed granulation [2–4], hot melt granulation [5], spheronization [6], and crystallization [7–9]. However, differences between the measurement mechanisms and principles of the particle size analyzers (both offline and in-process) make the direct comparison between them a challenging task [7,10]. The aim of this paper is to review different in-process particle sizing techniques and compare them to acknowledged off-line techniques (laser diffraction (LD) and sieve analysis). To establish this comparison, six batches of granules and pellets (i.e., spherical particles) having different sizes were measured with the different equipments. The evaluated in-process techniques include Focused Beam Reflectance Measurements (FBRM), Spatial Filtering Velocimetry (SFV), Photometric Stereo Imaging, and the Eyecon® technology. Table 1 provides a comparison between the assayed equipments. It discloses the

* Corresponding author. Faculty of Pharmaceutical Sciences, Laboratory of Pharmaceutical Process Analytical Technology, Ghent University, Harelbekestraat 72, B-9000 Ghent, Belgium. Tel.: +32 9 264 80 97; fax: +32 9 222 82 36.
E-mail address: Thomas.DeBeer@UGent.be (T. De Beer).

0939-6411/$ - see front matter © 2013 Elsevier B.V. All rights reserved.
http://dx.doi.org/10.1016/j.ejpb.2013.03.032

underlying theoretical assumptions behind each instrument's measurement mechanism, unveils the way in which size is acquired and presented by each instrument, describes their applicability, known capabilities and drawbacks. The choice of an appropriate analyzer for measuring particle size in a specific case has to take into consideration these listed characteristics. In an industrial environment, when a new particle size analyzer is implemented in a process environment, an often executed procedure is to attempt to correlate the data from the traditionally used off-line analyzer with the data from the new in-process analyzer. However, due to the different measurement principles behind each sizing technique, it is obvious that this is not an accurate and reliable procedure as mostly very different particle properties are measured by each sizing technique, hence providing uncorrelated results. A particle size distribution is usually depicted by a histogram where the size-related property measured by the analyzer (total particle volume, number of particles or counts, total particle length, total particle area, etc.) is plotted as a function of demarcated size classes. *D* values are parameters often used in the characterization of a PSD, a *Di* value of *x* indicating that particles with a size smaller or equal to *x* account for *i*% of the measured size-related property.

1.1. Off-line particle sizing methods

1.1.1. Laser diffraction

LD is the most applied technique for the particle size measurement of pharmaceutical powders and granules. It can be used as an in-process method [11] or as an off-line method. A dispersed sample passes through a beam of monochromatic light causing light scattering, which is measured as a function of scattering angle by a multi-element detector. As the scattering pattern, i.e., scattered intensity as a function of scattering angle, is largely particle size dependent, it follows that particle size information can be extracted from the experimentally determined pattern. Older instruments mainly rely on the Fraunhofer approximation to derive particle size information from the scattering pattern, while recent LD particle size analyzers are based on Mie's theory [10]. The Fraunhofer approximation is based on a number of assumptions: it assumes that particles are opaque disks, that light is scattered at only narrow angles, and that all particle sizes scatter with the same efficiency. Furthermore, it does not take into consideration the optical properties of the measured material, and therefore, its use is recommended when measuring mixtures of different materials. Differently, Mie's theory predicts the scattering intensity induced by particles, irrespective of the fact whether they are transparent or opaque. It is based on the assumptions that the measured particles are spherical, that the dispersion is dilute, so that light is scattered by one particle and detected before it interacts with other particles, that the optical properties of the particles and the medium surrounding them are known and that particles are homogeneous i.e., uniform in composition. Nowadays, the ISO13320 standard for LD particle size analysis acknowledges the superiority of Mie's theory [12,13]. LD particle size analyzers that use Mie's theory (e.g., Mastersizer® S) base their particle size calculation on the assumption that particles are spherical, which is rarely true. This is a solution to deal with the fact that the only shape that can be described by a single dimension is the sphere. LD results are generally presented as a volume-weighted particle size distribution. Thus, LD results reporting that the median value (D_{50}) of a volume-based PSD is 100 μm means that particles with a size up to 100 μm account for 50% of the measured sample volume. Alternatively, a number-weighted distribution can be extracted, depending on the analyzer's software.

1.1.2. Sieve analysis

Before the introduction of LD, sieving used to be the most commonly applied sizing method, and it is still widely used for the determination of particle size because of its inexpensiveness. It is described in the European Pharmacopoeia [14] that sieve size is the "size of the aperture measured perpendicular to the wire through the center of the opening." The mass of material that is retained on a specific sieve is weighted and presented as a percentage of the total assayed material. Therefore, a mass-based PSD is generated. The results are generally presented as a cumulative mass distribution. In this case, a median (D_{50}) of 100 μm indicates that 50% of the total weight of the measured material is constituted by particles that would pass through a sieve with 100 μm apertures. It is acknowledged that for a particle to pass through a sieve, it must have two dimensions smaller than the sieve size. This is why it can be assumed that sieve analysis separates particles according to their second largest dimension. Some of the described disadvantages of sieve analysis are as follows: test sieves require regular care in order to maintain their performance, their cleaning must be careful as vigorous brushing may distort sieve openings, it is not possible to perform sieve analysis on sprays or emulsions, measurement of dry powders with sizes under 38 μm is very difficult as electrostatic charges may cause loss of material (wet sieving may be a solution but this technique provides very poor reproducibility and is difficult to carry out), and cohesive or agglomerated materials are problematic to measure as they form aggregates that will not pass through the sieve's aperture [10,15]. Sieve analysis also requires a relatively large amount of sample and, as a consequence, is not appropriate for costly materials or materials of which only small quantities are available. Samples can be eroded due to attrition during the analysis making sieving unsuitable for these materials. Measurement times and operating methods (e.g., shaking) need to be standardized as the longer the measurement is performed, the smaller the obtained particle size is as particles have time to orient themselves to fall through the sieve. This is particularly important when dealing with odd-shaped particles which are difficult to sieve and may generate peculiar results. For instance, measuring the particle size of needle-like or rod-like particles by means of sieve analysis might not be the best choice. Additionally, there is an increase in the risk of particle erosion as sieving time increases. These and further disadvantages of this method are described in Table 1.

1.2. In-process particle sizing methods

1.2.1. Methods based on chord length measurements

There are in-process particle size analyzers that measure chord length instead of actual particle size such as SFV and FBRM. A particle's chord length can be defined as a geometric line segment whose endpoints both lie on the surface of the particle. These analyzers utilize a laser beam that crosses the particle randomly acquiring a chord length. The number of times a given chord length is measured takes the form of a probability density function. In case of spherical particles, the diameter is the largest chord possible, and the probability of the measured chord length is independent of the particle orientation toward the laser beam (Fig. 1-1), while for irregular and odd-shaped particles, shape and orientation will influence the measured chord lengths (Fig. 1-2a and 1-2b). Hence, the chord length distribution (CLD) depends on both the PSD and the particle shape. Presenting the results as particle size is easier to interpret than chord length as particle size is often directly related to product quality, and it allows the comparison to particle size measured by other instruments [16]. Both SFV and FBRM utilize a laser beam for their measurements: SFV calculates the chord length from the shadows cast by the particles that cross the laser beam, and FBRM calculates it from the laser light that is

Table 1
Comparison between the different studied particle size analyzers (CL – chord length; CLD – chord length distribution; N/A – non-applicable; PS – particle size; PSD – particle size distribution).

Instrument	Mastersizer® S (LD)	Sieve analysis	Parsum® IPP70 (SFV)	FBRM® C35	FS3D® (Photometric Stereo Imaging)	Eyecon®
Assumptions	Mie's theory: Assumes particles to be spherical|Assumes scattered light is measured before it is re-scattered by other particles|Optical properties of the particles and the medium surrounding them are supposed to be known [13]	Particles will pass through the mesh when the second largest dimension is less than the mesh size, i.e., at least two dimensions of the particle must be smaller than the sieve size	No assumptions about particle shape are made	No assumptions about particle shape are made|Particle velocity is small compared to the laser rotational velocity [16,29,30]	Samples are positioned against a straight glass and therefore the surface is assumed to be approximately straight. Linear integration in a horizontal direction which allows the obtention of a 3D surface. Peaks on this surface are assumed to be particles [41]	An ellipse is fitted to the particle edges in order to obtain an average particle diameter|Assumes particle as being spherical to allow the calculation of its (relative) mass from the average diameter, this mass is used in the calculation of D values
Size distribution type	Volume-based PSD	Mass-based PSD	Volume or number-based PSD (obtained by conversion from a CLD)	CLD (possible to apply different weighting methods)	Volume-based PSD	Number-based PSD
PS interval	0.05–3500 μm	>38 μm [10]	50–6000 μm	3–3000 μm	>20 μm (maximum size depends on the performed calibration) [41]	50–3000 μm
Particle velocity	N/A	N/A	0.01–50 m/s	N/A	N/A	N/A
Destructive	Sample can be retrieved but sample dispersion by means of pressurized air may cause particle breakage [3]	Yes	No	No	No	No
In-process measurements	Not with Mastersizer® S. Possible with some equipments (Insitec® by Malvern, UK; Mytos ® by Sympatec, Germany) but difficulties on presenting the sample in the appropriate concentration [11]	N/A	Yes (bench-top version also available)	Yes	On-line measurements are possible with appropriate feeder (however the measured sample has to be static)	Yes (bench-top version also available)
Suitable for	Non-fragile particles (powders or liquid suspensions or emulsions)	Powder or granular solid particles >38 μm	Solid particles suspended in an air stream	Solid particles suspended in a liquid or in an air stream	Solid particles	Solid particles
Advantages	Ease of use|Little maintenance|Rapid measurements|Highly repeatable|Allows background subtraction|No calibration required [13]	Cheap	Ease of use|Little maintenance|Rapid measurements|No calibration required|Shape is taken into consideration [18,21]|Probe fouling is prevented by means of a pressurized air system|Clip-in accessories are available for measurements under difficult process conditions	Ease of use|Little maintenance|Rapid measurements|Shape is taken into consideration|In this model a window scrapper allows measurements in highly concentrated particle systems	Ease of use|Little maintenance|Rapid measurements|Provides particle size alongside with important morphological information|Able to image overlaying, wet particles and extract PSD	Ease of use|Little maintenance|Rapid measurements|Provides both size and morphological information under dynamic conditions
Disadvantages	Relatively large amount of sample required for dry dispersion method (depending on the size of the particles)	Cohesive and agglomerated materials are difficult to measure|Low resolution due to the limited amount of sieves that can be fitted| Measurement times and operating methods have an	Property being measured is CL and not PS (conversion to PSD by the instrument's software)|Not suitable to measure sizes <50 μm|Probe may be susceptible to fouling [20] |Accessories are adequate	Property being measured is CL and not PS [30,44,47,48]	Samples have to be static |Shades caused by irregularities in the surface of a particle may trick the instrument in detecting multiple particles [41]|Transparent particles	At the moment no information available about performance during in-line measurements

Table 1 (*continued*)

Instrument	Mastersizer® S (LD)	Sieve analysis	Parsum® IPP70 (SFV)	FBRM® C35	FS3D® (Photometric Stereo Imaging)	Eyecon®
		influence on the results|Particle shape has a big influence on the results|Laborious and time-consuming| Requires large amount of sample [10]	only within a particle size range, if particles are outside this range they are not measured thus providing biased results		cannot be measured|Coverage of the measurement window by fines at the moment of sampling may lead to particle size underestimation [41,46]	

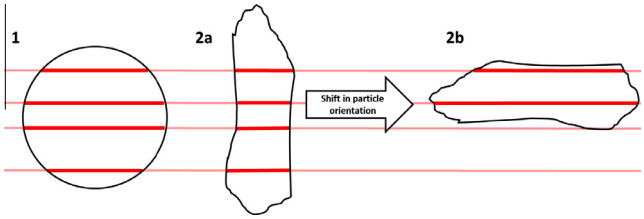

Fig. 1. Examples of the measured chord length (bold line) when a laser beam crosses (1) a spherical particle and (2a and 2b) an irregular particle in different positions – illustration of the effect of particle orientation on the obtained chord length. (For interpretation of the references to color in this figure legend, the reader is referred to the web version of this article.)

reflected back from the particle and propagated back through the probe.

1.2.1.1. Spatial Filtering Velocimetry. A system based on the SFV principle is the Parsum® IPP70 probe which was utilized in this study. The working principle of the Parsum® IPP70 SFV probe is presented in Fig. 2. When passing in-between the two sapphire windows of the probe, the laser beam hits the particles. These particles cast then a shadow on a detector array of optical fibers generating two burst signals (*burst a* and *burst b*). The difference between these two bursts is obtained (“BURST”), and its frequency calculated. This frequency (f) is then multiplied by the spatial filter constant (g), which corresponds to the distance between the detector arrays, and the particle’s velocity is obtained (v). When the particle travels through the probe, a secondary signal (“PULSE”) is also acquired by a single optical fiber, and the duration of this pulse is measured (tp). The chord length (x) of the particle is then calculated by multiplying the particle’s velocity with the pulse signal’s duration [17–19]. The Parsum® IPP70 system is able to report size after converting the raw CLD to a number or volume-based PSD performed by an algorithm in the system’s software. Some of the algorithms that have been described to convert from a CLD to a PSD are addressed later on in Section 1. Furthermore, the user is allowed to define the different size classes. In this way, the percentage of particles with sizes in-between the user-defined values is calculated. Fouling is a recurrent problem during in-process measurements, and for that reason, the sapphire windows of the Parsum® IPP70 probe are kept clear by feeding compressed air through the probe itself, though this is not always efficient [20]. Additionally, a range of different clip-in accessories is available. Two different flushing cells: SZ11 (an open flow cell slit) and SZ20-4 (a cell with a front side aperture of 6 mm), both designed to protect and keep the probe’s windows clear. According to the manufacturer’s specifications, the SZ11 is appropriate for the measurement of free-falling particles with sizes between 100 and 4000 μm and a very low percentage of fines, whereas the SZ20-4 is suitable for measuring free-falling particles with sizes from 50 to 2500 μm and a low to average content of fines. A disperser accessory with a ring injector, diluter, and a back flush function aperture of 4 mm (D23) with both an external and internal air connection is also available and is particularly fit for the measurement of small particles (50–2000 μm), especially in processes with high particle concentrations in the measurement volume, i.e., high particle loadings. Parsum® IPP70’s software enables the monitoring of particle loading during measurements expressed as a percentage of the measurement volume. By the use of the disperser D23, particles are accelerated, and consequently, the distances between them become larger ensuring that they are presented to the instrument’s detector in a suitable concentration for an accurate measurement. The choice of the appropriate accessory to utilize depends on the characteristics of the particles being analyzed.

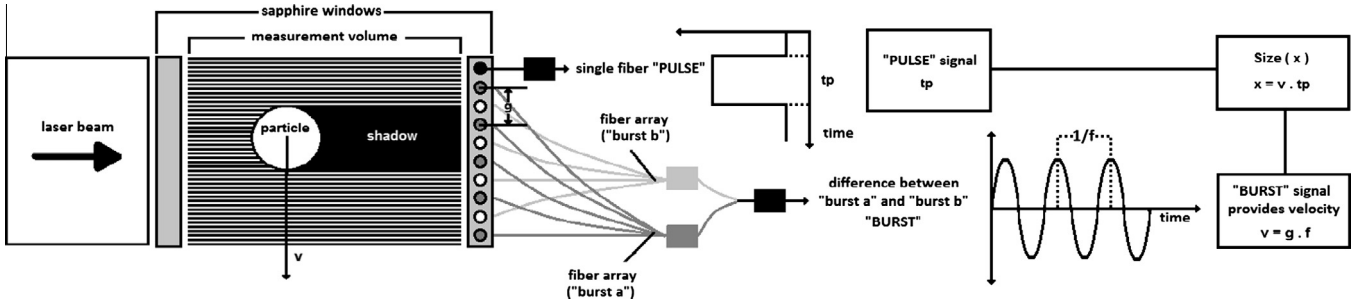

Fig. 2. Working principle of the Parsum® IPP70 probe.

For instance, the measurement of a sample containing particles outside the appropriate size range for a certain accessory will result in biased results. SFV has already been suggested for particle size monitoring in fluidized bed processes [2], mixing and coating, high shear wet granulation, dry granulation, and spray-drying [21].

1.2.1.2. Focused Beam Reflectance Measurements. FBRM is another process analytical tool designed for measuring chord lengths. It measures the light that is reflected and propagated back through the probe when a tightly-focused laser beam, rotating at a high speed (2–8 m/s), hits a particle (Fig. 3). The chord length is then calculated by multiplying the duration of reflection with the laser beam's scan speed. FBRM has already been successfully applied for suspensions and crystallization processes [7–9,22–24] and has also been studied for fluid bed granulation in comparison with other PAT tools [25]. Polymorphic transition monitoring [26], control of particle disruption [27], and solubility measurements [28] are some other applications where the use of FBRM has already been reported. FBRM® C35 measurements can be performed in highly concentrated particle systems as a scraping system is installed on the probe's sapphire window, keeping it clean and preventing probe fouling during in-process measurements. FBRM® C35 is a count-based technique which means that the sizing results are presented by the FBRM® C35 software (iC FBRM®) as a number-based chord length distribution (number of particles measured within a chord length class). This software also allows the extraction of *D* values from these distributions and of size (chord length) classes. As mentioned previously, size results are usually presented as a number, length, area, or volume-based distribution. However, the FBRM® C35 system results are presented as a raw chord length frequency distribution and can be transformed into a 1/length-weighted, length-weighted, square-weighted, or cubic-weighted chord length frequency distribution. The weighing method to use depends on the aim of the measurement. If there is the necessity of detecting slight changes in the fraction of smaller particles, no weighing or length-weighing will emphasize these rather than the larger ones. On the other hand, if the interest lies on detecting small changes in the larger particles square and cubic weighing emphasize the coarser particles at the same time making the detection of changes in the smaller size range more difficult. It is described that the raw chord length data are similar to a length-based PSD since the probability of a certain chord length being detected is proportional to the linear dimension of a particle.

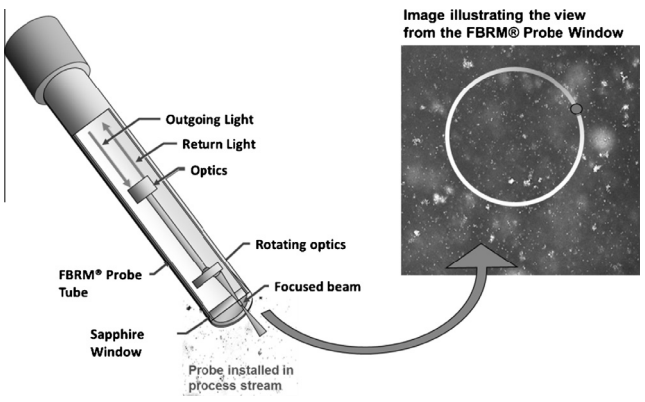

Fig. 3. Working principle of the FBRM® technology [44].

SFV and FBRM both measure chord length, but their measuring principles differ substantially. For the FBRM® C35 system, it is necessary for particles to flow over the sapphire window. Particles that are positioned a few hundred micrometers away from the sapphire window will most likely not be measured, hence making the placement (implementation in the process environment) of the FBRM® C35 probe of utmost importance. Dispersing and measuring the sample in a liquid in which it is insoluble is a highly suitable solution for the FBRM® C35 system. However, the sample has to be diverted from the process and is not reusable. Parsum® IPP70 or any other SFV system cannot be applied in suspensions. FBRM® C35 is capable of measuring smaller particle sizes (i.e., 3–3000 μm), while SFV is adequate for the measurement of particle systems sized 50–6000 μm. The main advantages of using these systems include the fact that no calibration is needed and the capability of measuring in-line at high particle concentrations (loadings) due to the use of purging systems [29,30].

As a particle chord length is not identical to the generally used particle size, several authors have presented their solutions to express the relationship between PSD and CLD. The Parsum® IPP70's software performs this CLD–PSD conversion itself, while for the FBRM® C35, the results are expressed as chord lengths. The easiest way to convert a CLD into its corresponding PSD is by developing a PSD–CLD model to calculate CLD corresponding to a known PSD and shape and afterward invert it to obtain a PSD from the CLD (CLD–PSD model) [16]. For 2-dimensional spherical particles, the translation from PSD to CLD is based on different methods such as the probability apportioning method and Bayes' Theorem [31–35]. The probability apportioning method can also be used to calculate CLD from PSD for 2-dimensional ellipsoidal particles [35–38]. For non-spherical 2-dimensional and 3-dimensional particles, little has been described [35,39]. In 2001, Langston and Jones [39] presented a method in which for a certain PSD of non-spherical particles, the chord length probability distribution is determined by simulating random cuts in the particles. This method is highly dependent on assumptions made during the calculation, and the resulting data are not accurate. On the other hand, Ruf et al. [30] presented another procedure in which, for a 3-dimensional ellipsoidal particle, the chord length probability distribution is obtained from 2-dimensional projections at every orientation. The conversion of a PSD from a CLD is an inversion problem, and the most utilized methods to solve this problem include the Least Squares and Constrained Least Squares algorithms [31,33,34,37,38,40]. However, these might provide negative numbers of particles when the CLD

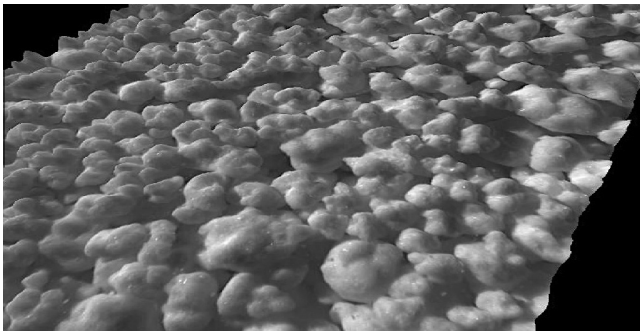

Fig. 4. A typical example of a surface visualized in 3D that is used in particle sizing with the photometric stereo approach.

measurements are noisy, and therefore, an interactive apportioning method utilizing Bayes' Theorem has been developed to overcome this limitation [34,31]. For most processes, however, a good precision is often more important than accuracy as the interest relies on the monitoring of process dynamic changes such as particle shape and/or concentration of the suspensions [16,30].

1.2.2. Photometric Stereo Imaging

Another studied technique was Photometric Stereo Imaging. The Photometric Stereo Imaging unit Flashsizer3D® (FS3D®) consists of a monochrome CCD camera connected to a metal cuvette with a glass window and a computer. The tool is equipped with a sampling unit that allows online measurements. Two light sources, positioned relative to each other at an angle of 180°, illuminate the sample, and two digital images of the sample are obtained. A gray-scale value between 0 (black) and 255 (white) is attributed to each individual pixel, and the shading effects expose the topography of the surface (Fig. 4). The gradient fields are subjected to line integration in a horizontal direction to obtain a 3D surface. This surface is assumed to be approximately straight as the samples are placed against a straight glass surface during measurement. Therefore, peaks on the 3D surface are assumed to be particles, and the projected volume-based (V) particle size is then calculated from the area of the peaks in the xy direction:

$$d = \sqrt{(a)} \cdot c \tag{1}$$

$$V = d^3 \tag{2}$$

where d is the diameter of the particle, a is the area of the peaks and c a calibration constant, calibrated by default with pellets [41]. If the shape of the particles to be measured differs significantly from spherical, the calibration constant can be changed accordingly to the particles to be measured [26]. This imaging unit allows the acquisition of a volume-based PSD and related D values of the particles captured in each image. The size classes can be defined by the user. The FS3D® system has been used for the measurement of powders [42], granules [41], and pellets [6] showing the potential of this technique as a fast particle size analyzer for various types of material.

1.2.3. Eyecon®

The Eyecon® particle sizing technology was also tested. This is a very recent 3D-imaging system that allows the determination of the PSD for moving particles using a flash imaging technique (Fig. 5). The equipment can either be used offline or in-process. During measurements, a powerful short light pulse is created and provided that the particle movement during this pulse is negligible a sharp image without blurring is captured. The particles are illuminated with red, green, and blue LEDs from different angles. The color on the surface of the particle is captured in an image, and for each individual pixel, a map of the surface height is built. Furthermore, using image gradient data an ellipse is fitted on the particle edges, and its maximum and minimum diameters are obtained. These are used to calculate the average aspect ratio (AAR) of particles as an indicator of their sphericity by means of the following equation:

$$AAR = \frac{D_{max}}{D_{min}} \tag{3}$$

where D_{max} represents the maximum measured diameter and D_{min} the minimum measured diameter. Also, the average diameter can be assessed according to the following equation:

$$d = \frac{D_{max} + D_{min}}{2} \tag{4}$$

Posteriorly, the particle is modeled as a sphere, and its mass is obtained by means of following equation:

$$M = \frac{\pi \cdot d^3 \cdot \rho}{6} \tag{5}$$

where ρ represents the density of the particles. As it is an unknown value, all the particles are assumed to have the same density, and therefore, it is a constant that can be eliminated, as can π and 6 and Eq. (6) is obtained:

$$M = d^3 \tag{6}$$

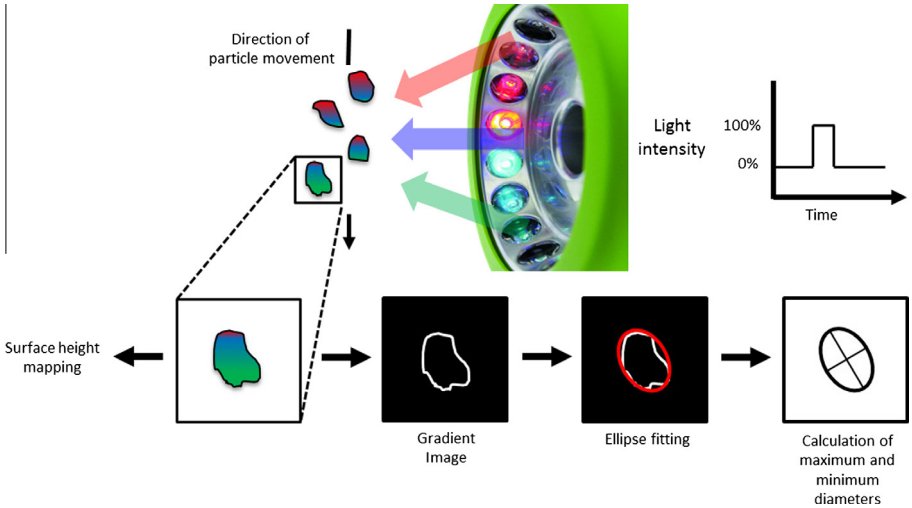

Fig. 5. Working principle of the Eyecon® equipment. (For interpretation of the references to color in this figure legend, the reader is referred to the web version of this article.)

The obtained mass value is then a relative mass value, not a true mass. Each captured image is analyzed by Eyecon® resulting in a group of ellipses. Results can either be computed using only the current image or also include data from previous images and are presented as a histogram.The *D* values are calculated by ordering particles in order of ascending relative mass. Firstly, the total mass is computed, and then, an iterative algorithm adds up starting with the smallest of the particles. As the running total reaches 10%, 25%, 50%, 75%, and 90% of the total mass, the diameter of the last added particle is recorded as being the D_{10}, D_{25}, D_{50}, D_{75}, and D_{90} diameter, respectively.

2. Materials and methods

2.1. Materials

Six different batches of particles were used in this study. Three of them were granules of different sizes prepared in a laboratory-scale fluid bed granulator (GPCG 1, Glatt, Binzen, Germany). These batches consisted of 700 g of dextrose monohydrate (Roquette Frères, Lestrem, France) and 277.5 g of unmodified maize starch (Cargill Benelux, Sas van Gent, the Netherlands) and were granulated with an aqueous binder solution of 20 g HPMC (Dow Chemical Company, Plaquemine-LA, USA) and 2.5 g Tween 20 (Croda Chemicals Europe, Wilton, United Kingdom), sprayed as a 4% (w/w) solution. The three granulations were performed varying the process parameters: inlet air temperature during the spraying phase, spray rate and inlet air temperature during the drying phase, in order to obtain batches with different granule sizes (Table 2). The remaining three batches consisted of commercially available microcrystalline cellulose spherical pellets of different sizes commonly known as Cellets® (Cellets®, Pharmatrans Sanaq Pharmaceuticals, Basel, Switzerland). The selected pellet sizes were Cellets® 350 (350–500 μm), Cellets® 500 (500–710 μm) and Cellets® 1000 (1000–1400 μm). Images of the three granule and three pellet batches were obtained using the FS3D® equipment (Fig. 6).

Table 2
Process parameters varied on the performed granulations.

	Inlet air temperature during the spraying phase (°C)	Spray rate (rpm)	Inlet temperature during the drying phase (°C)	Median particle size (D_{50}) obtained with Mastersizer® S (μm)
b1	30	22	50	193
b2	30	36	70	383
b3	40	29	60	207

2.2. Methods

2.2.1. Off-line methods

2.2.1.1. Malvern Mastersizer® S. Samples from each batch were measured twice using the LD equipment (Mastersizer® S long bench, Malvern Instruments, Malvern, UK) by means of three different methods: dry dispersion, wet dispersion, and free fall experiments. In all cases, the 1000F lens was utilized, the particle size analysis of each sample was performed using 10,000 sweeps, and the obtained particle obscuration was comprehended between 10% and 30%.

In the dry method, the MS-64 sample dispersion analyzer was utilized. Two air stream pressures to aid with sample dispersion were tested (1 and 3 bars). For the wet method, Miglyol 812 (Fagron, Capelle aan den IJssel, the Netherlands) was chosen as dispersant given that both types of particles are insoluble in this liquid. The diluted dispersion was recirculated from the small volume sample adaptor through a flow cell using a peristaltic pump. In the free fall method, the sample was fed by a vibratory feeder (DR100, Retsch, Haan, Germany) to an in-house free fall controlled flow unit. At the end of this unit, a vacuum cleaner (GS80, Nilfisk, Brøndby, Denmark) was placed to collect the sample and so avoid repeated measurements of the same particles.

PSD was estimated using standard reference indexes and by way of an algorithm based on Mie's theory, provided with the diffractometer. The granule batches were analyzed as polydisperse and pellet batches as monomodal. When measuring the pellet particles with sizes around 1000 μm and larger (Cellets® 100) via the wet dispersion method, the background signal was already very high due to the combination of the lens and the use of Miglyol as the dispersant. In order to overcome this experimental difficulty, the signal at the first channels was discarded with minimal influence in the accuracy of the results.

2.2.1.2. Sieve analysis. Sieve analysis was performed, in triplicate, on 20 g of sample from each batch. Nine sieves with mesh sizes of 2000, 1400, 1000, 500, 315, 250, 180, 100, and 50 μm were stacked. A collector pan was placed below the sieve with the smallest mesh size. The samples were placed on the top sieve (2000 μm) and a lid was placed on it. The assembly was vibrated on an automatic sieve shaker (VE 1000, Retsch, Haan, Germany) for 5 min with an amplitude of 2 mm. Such gentle conditions were chosen

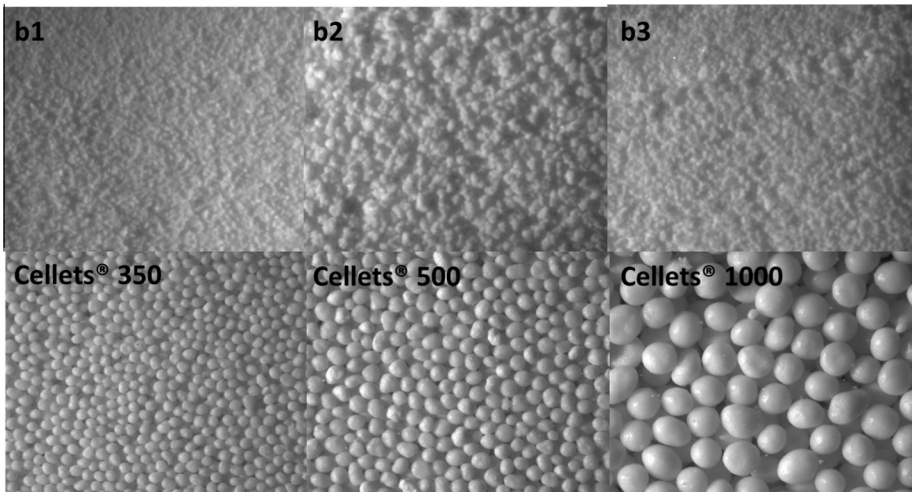

Fig. 6. Pictures of the assayed granules and Cellet® batches taken with the FS3D® equipment.

to prevent breakage of the granule samples. After shaking, each sieve was weighted individually and the mass percentage of material retained on each sieve was calculated.

2.2.2. In-process methods

2.2.2.1. Parsum® IPP70. The six different particle batches were fed to the measurement zone of the SFV probe (Parsum® IPP70; Gesellschaft für Partikel-, Strömungs- und Umweltmesstechnik, Chemnitz, Gemany) by means of a vibratory feeder (DR100, Retsch, Haan, Germany) to simulate in-line measurements of a process's particle flow stream. The disperser accessory with a ring injector (D23) was employed during the size determination of the three granule batches in order to facilitate the measurement of the smaller particles. This cell was operated with an internal (15 L/min) and external (3 L/min) pressurized air connection. The open flow cell (SZ11) was used for the measurement of the pellet batches, working with a pressurized air stream of 4 L/min. SFV measurements were taken every 10 s for a period of 5 min. Six replicate measurements were performed for each batch, on six different days. After the analysis of the acquired size distributions and *D* values, it was found necessary to perform an extra series of measurements where the particle loadings were controlled (see results and discussion). Six replicate measurements of each batch were performed. Data were acquired every 10 s for a period of 5 min.

2.2.2.2. FBRM® C35. A small quantity of granules (2.5 g) or pellets (3.5 g) was added to a beaker containing 40 ml of Miglyol 812 (Fagron, Capelle aan den IJssel, the Netherlands). The FBRM probe (FBRM® C35, Mettler-Toledo AutoChem, Columbia, MD, United States) was immersed in the suspension at an angle of approximately 45° to allow optimum sample presentation [43]. A magnetic stirrer was used to gently agitate the suspension without breaking down the granules. FBRM measurements were performed every 10 s, during a period of 3 min. The six batches were measured in triplicate, on three different days. The size information was extracted through the iC FBRM® 4.0 software (Mettler-Toledo AutoChem Inc., Columbia, MD, United States).

2.2.2.3. Flashsizer® 3D. The particle size of the six batches was assessed six times on six different days. The samples were filled into a petri dish and positioned on top of the imaging instrument's (Flashsizer 3D®, FS3D®, iPAT Ltd., Turku, Finland) glass window. Two digital images were captured during each measurement and combined to obtain a 3D surface from which the relevant particle size information was calculated.

2.2.2.4. Eyecon®. The Eyecon® 2D and 3D particle imager (Eyecon®, Innopharma Labs®, Dublin, Ireland) was used offline. As particle movement during the light pulse is negligible, in theory, results obtained offline will be similar as when the measurements were performed in-process. One sample was collected from each batch and placed on a petri dish. Twenty images were taken from each individual sample, and an average of the PSD parameters of interest was calculated.

2.2.3. Acquired particle size parameters

As mentioned previously, from sieve analysis, mass-based sieve fractions were obtained. On the other hand, FS3D®, Parsum® IPP70 and FBRM® C35 equipments allowed the definition of size or chord length classes. Sieve fractions were first chosen for sieve analysis, and afterward, the same sieve sizes were introduced in each instrument's software (with the exception of Eyecon® where this feature is not available). The selected sieves (size classes) 50 μm, 100 μm, 180 μm, 250 μm, 315 μm, 500 μm, 715 μm, 1000 μm, 1400 μm and the related *D* values D_{10}, D_{50}, and D_{90} were acquired from each individual instrument's software. For sieve analysis, *D* values were calculated from the sieve distributions by linear interpolation of the obtained cumulative mass percentage curve, while for the other techniques, the instrument's software directly provided these results.

3. Results and discussion

The comparison between the particle size information obtained from the different studied particle sizing techniques is not straightforward since each technique is unique in its way of measuring and calculating size. Not only the underlying measurement method might have an influence on the acquired particle size (or chord length), but also the algorithms used for obtaining particle size information from the measured particle properties and the way in which size results are presented are essential. Sieving results are mass-weighed, while volume-weighed data are obtained from Mastersizer® S and FS3D®. Eyecon®'s *D* values are based on relative mass values. The chord length measurements performed with Parsum® IPP70 are converted by the instrument's software to a volume-weighed particle size distribution. Square-weighted chord length distributions were obtained through FBRM® C35 as it has been previously described by Heath et al. [44] that these data present the best agreement with the particle size distribution obtained from LD measurements. FBRM measures the first diameter weighing of the chord distribution, and it is then effectively a cube (volume) weighing which is comparable to the volume-based distribution obtained from laser diffraction. The sieve size distributions of each batch are represented in Fig. 7a–f and the related *D* values in Fig. 8a–c.

3.1. Choice of the reference method (Mastersizer® S)

Laser diffraction is often utilized as a reference for comparison with other sizing techniques [12,45]. Fig. 9 displays the D_{50} value of the six studied batches, obtained with Mastersizer® S using the different measurement methods. It was observed that particle sizes obtained from dry dispersion measurements of the granule batches were significantly smaller than the ones attained from the wet dispersion and free fall methods. When air pressure was augmented from 1 to 3 bars, this reduction in size was more pronounced. Therefore, we believe that the use of pressurized air as the dispersing agent damaged the fragile granules. In contrast, for the pellet batches (particles with a low friability), no meaningful size differences were observed between all methods. All in all, the results obtained for all batches for wet dispersion, and free fall experiments are very similar but the wet dispersion method presented a better precision. For that reason, Mastersizer® S wet dispersion method was used as the reference sizing technique for the rest of this study.

3.2. In-process methods and sieve analysis versus reference method

3.2.1. Parsum® IPP70

Both Mastersizer® S and Parsum® IPP70 present their results as volume-based particle size distributions. Nevertheless, it is important to always keep in mind that, differently from Mastersizer® S, Parsum® IPP70 does not measure particle size but chord, converting it afterward into a PSD by means of the instrument's software. The comparison between the *D* values obtained from the initial Parsum® IPP70 measurements and from the Mastersizer® S measurements is depicted in Fig. 10.

The *D* values attained with both techniques, Parsum® IPP70 and Mastersizer® S, for granule batches b1 and b3 (the batches with the smallest granule size) are perfectly in agreement. Differently, for batch b2 particularly, the obtained D_{90} value was larger for

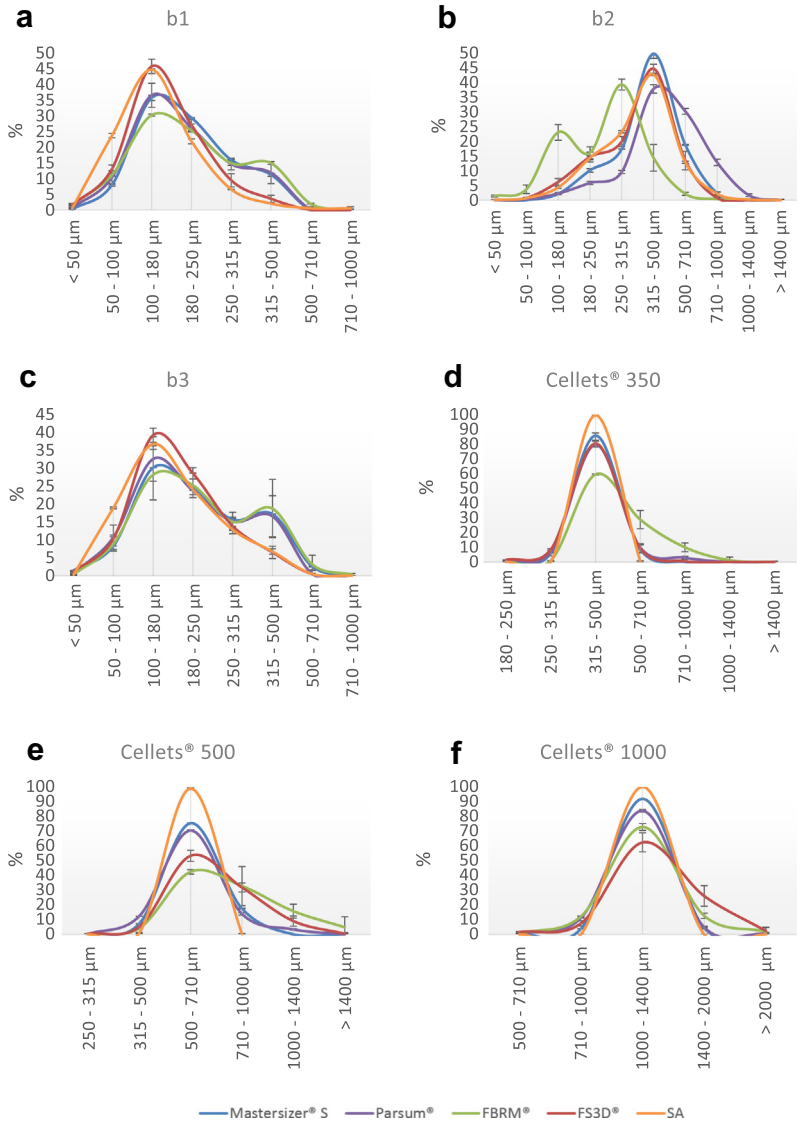

Fig. 7. Particle size distributions of the assayed batches obtained with the different equipments. (For interpretation of the references to color in this figure legend, the reader is referred to the web version of this article.)

Parsum® IPP70 than for Mastersizer® S. Looking into the results for pellet batches, it is observed that the D_{90} values are also larger when measured with Parsum® IPP70 and that this difference is more obvious with a larger particle size. All things considered the D_{90} values obtained with Parsum® IPP70 are mostly larger than the values obtained with Mastersizer® S which strongly suggests that these results could be a result of particle coincidence. If occasionally two particles cross the laser beam at the same time, the Parsum® IPP70 probe is not able to make the distinction between the two shadows of the different particles hence detecting as one large particle. Therefore, a falsely increased number of larger particles might be reported hence shifting the distribution toward larger sizes. The average particle loadings registered for this initial set of measurements (Fig. 10) are depicted in the first column of Table 3. It is observed that there are high loadings, which means that a high percentage of the measuring volume is at any time occupied with particles and, as these particles might overlap, the probability of errors by coincidence of particles is higher. To prove that high particle loadings might cause size overestimation in this system, two different measurements of each batch with a different average particle loading were performed. The different loadings per batch are depicted in the second column of Table 3. The obtained corresponding D values are portrayed in Fig. 11a and b. Batches b1 and b3 did not reveal a significant influence due to the increase in particle loading (Fig. 11a). However, as the size of particles increases (batch b2 and pellet batches, Fig. 11a and b), and with the increase in particle loading, the overestimation becomes more noticeable, especially for the D_{90} values. Particle coincidence due to high loadings is a complication which needs to be taken into account when performing measurements with the Parsum® IPP70 system. In the instrument's software, several settings can be altered in order to prevent this type of errors. For instance, a maximum loading level can be established and if at a certain time the particle loading exceeds the set maximum value, these data are not recorded. Also, a search for coincidence and removal can be activated by defining a coincidence level. This coincidence level is a user-set percentage of the highest size class of the acquired number distribution and, notionally, it should be as low as possible in order to achieve the maximum sensitivity. Concerning the Parsum® IPP70 equipment itself, especially in processes with small particles and high particle loadings, the use of the in-line disperser D23 is important and recommended in order to keep the loading low enough avoiding coincidence errors. Finally, Parsum® IPP70 and Mastersizer® S were compared utilizing the data acquired with the lowest recorded

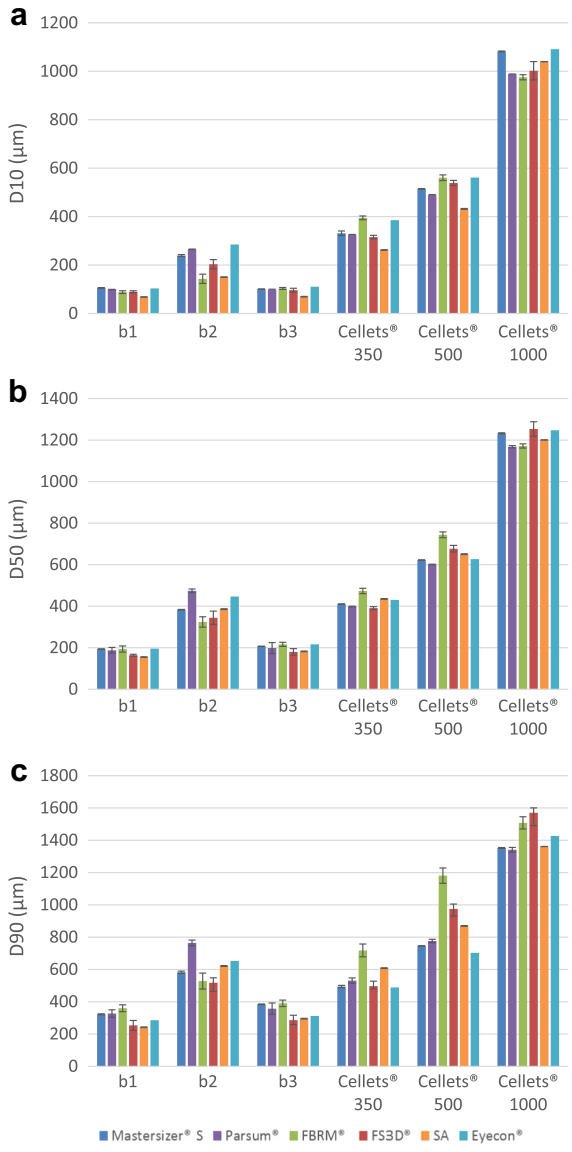

Fig. 8. *D* values of the assayed batches obtained with the different methods. (For interpretation of the references to color in this figure legend, the reader is referred to the web version of this article.)

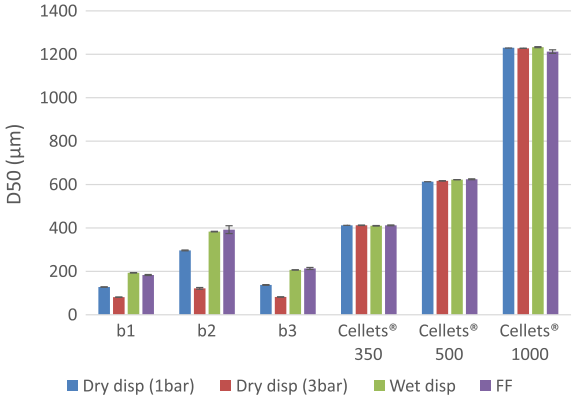

Fig. 9. Comparison between the D_{50} values of the assayed batches obtained with the. Mastersizer® S equipment by means of the dry dispersion (Dry disp), wet dispersion (Wet disp) and free fall (FF) methods. (For interpretation of the references to color in this figure legend, the reader is referred to the web version of this article.)

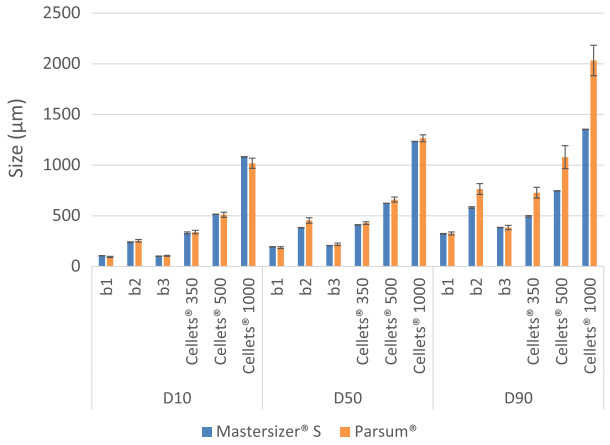

Fig. 10. *D* values of the assayed batches obtained with Mastersizer® S and Parsum® IPP70. (For interpretation of the references to color in this figure legend, the reader is referred to the web version of this article.)

Table 3
Average particle loadings for each batch in the performed Parsum® IPP70 measurements.

	Average loadings of the first set of measurements (%)	Low/high average loadings of the repeated measurements (%)
b1	6.84	3.65/11.38
b2	6.79	2.94/9.76
b3	7.09	2.6/9.05
Cellets® 350	16.57	3.1/13.7
Cellets® 500	16.09	2.6/16.71
Cellets® 1000	17.7	2.2/17.43

particle loading (Fig. 7a–f and Fig. 8a–c) to discard the differences that could arise from coincidence. Batches b1 and b3 presented similar size distributions when measured with both instruments (Fig. 7a and c) and, hence, also very similar *D* values (Fig. 8a–c). Regarding batch b2, all obtained Parsum® IPP70 *D* values were larger compared to the corresponding Mastersizer® S values (Fig. 8a–c). In the size distribution, a shift of the Parsum® IPP70 distribution toward larger sizes is observed when comparing to the Mastersizer® S's distribution (Fig. 7b). This shift is most probably related to a sampling difficulty rather than to an instrumental dissimilarity. Batch b2 presented a very broad size distribution, and it was possible to observe that the larger particles were the first to be directed from the feeder to the probe's measurement zone and into the aluminum tray, while some of the batch's fines were retained in the feeder not being measured. Concerning Cellets® 350 the *D* values (Fig. 8a–c) and size distributions obtained with Parsum® IPP70 and Mastersizer® S (Fig. 7d) are similar. Regarding Cellets® 500 and Cellets® 1000 size distributions from Parsum® IPP70 and Mastersizer® S are identical (Fig. 7e and f) as are the D_{90} values (Fig. 8c). However D_{10} and D_{50} are slightly larger for Mastersizer® S (Fig. 8a and b), specially for Cellets® 1000.

3.2.2. FBRM® C35

The size distribution curves of the batches with the smallest granules, b1 and b3, obtained with Mastersizer® S (volumetric particle size) and with FBRM® C35 (square-weighted chord length) (Fig. 7a and c) and the *D* values obtained from both techniques are very similar (Fig. 8a–c). This was expected as volume-based PSDs measured by LD, and square-weighted CLDs are predicted to be in good agreement for spherical particles [44]. However, in comparison with Mastersizer® S, the PSD measured using FBRM® C35 of the granule batch b2 is smaller (Fig. 7b) as are the *D* values (Fig. 8a–c). When looking at the obtained particle size distributions (Fig. 7b), a major shift toward

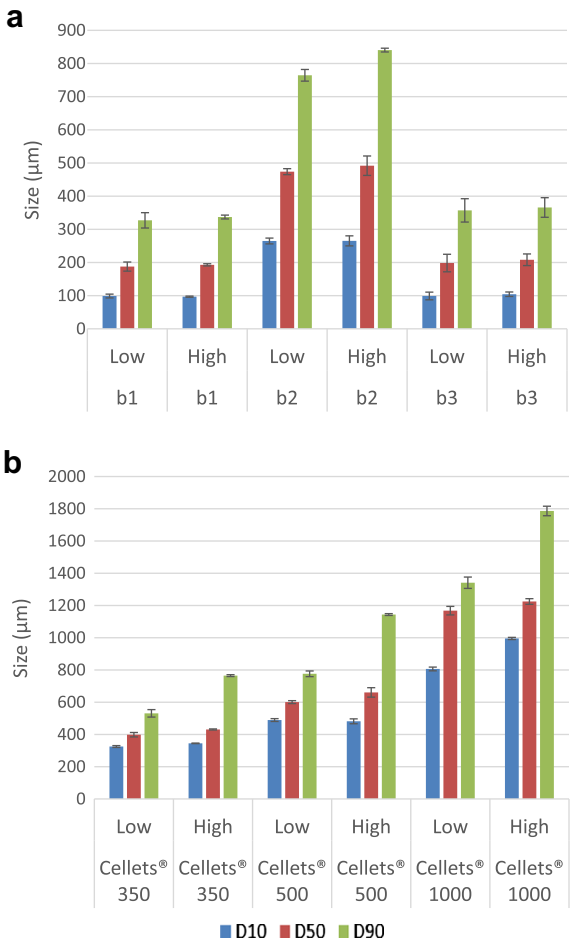

Fig. 11. *D* values of the Parsum® IPP70 measurements performed at different particle loadings (see Table 3 for further information on loadings). (For interpretation of the references to color in this figure legend, the reader is referred to the web version of this article.)

smaller sizes is visible. The agitation needed and used to keep the particles in suspension (see materials and methods) might have been responsible for their breakage. Pellet batches Cellets® 350 and Cellets® 500 were overestimated by FBRM® C35 when comparing to Mastersizer® S (Fig. 7d and e) resulting in larger *D* values, particularly D_{90} (Fig. 8a–c). It is possible that when performing the measurements for these batches, particles were too close together causing a phenomenon of chord concatenation i.e., an error by coincidence of particles. This type of error occurs when two particles cross the laser beam so close together that the analyzer cannot individualize them and counts two particles as one. For batch Cellets® 1000, the distributions from both analyzers are in good agreement though, as expected, the square-weighted CLD obtained from FBRM® C35 is wider than the volume-based PSD acquired with Mastersizer® S (Fig. 7f) resulting in a smaller D_{10} and a larger D_{90} (Fig. 8a and c). One must always keep in mind that no perfect correspondence between an unweighted or weighted CLD and PSD is achievable and converting from CLD to PSD (as in the case of the Parsum® IPP70 equipment) by assuming a certain particle shape might be a suitable solutions for simultaneous comparison of results from instruments that measure chord length with instruments that determine particle size.

3.2.3. Flashsizer® 3D

Both FS3D® and Mastersizer® S present their results as volume-based PSDs though they possess distinct underlying methods for calculating the particle size. In comparison with the Mastersizer® S results, the particle size of granule batches measured with FS3D® was underestimated (Fig. 7a–c), presenting slightly smaller D_{10}, D_{50} and D_{90} values (Fig. 8a–c). The irregularities of the particles that present a rough surface (as is the case for the granules) may cast shades which are interpreted by the instrument as being the edges between two particles, consequently causing particle size underestimation. This phenomenon has been previously described [42]. Another possible explanation for the observed underestimation is that, when there is a relatively large amount of fines, during the sampling procedure these can cover the measurement window preventing the measurement of the larger particles [46]. Cellets® 350 size distributions (Fig. 7d) and *D* values (Fig. 8a–c) for both instruments were in good agreement but, for the Cellets®500 and Cellets® 1000, an overestimation of the larger particles was observed in comparison with Mastersizer® S (Fig. 7e and f) with significantly larger D_{90} values obtained for FS3D® (Fig. 8a–c). An explanation for this phenomenon is that as particle size increases fewer, and fewer particles are measured per image, and statistically, a reduced number of large particles can greatly influence a volume-based particle size distribution shifting it toward the larger end of the distribution.

3.2.4. Eyecon®

Eyecon® and Mastersizer® S use different measurement principles and algorithms for the calculation of particle size. From Eyecon®, it is possible to extract a number-based size distribution (number of particles versus the average diameter) divided into several classes. However, the user cannot set these classes himself, and consequently, it was not possible to plot the results altogether with the size distributions obtained with the other equipments. Therefore, the comparison between Eyecon® and Mastersizer® S is established regarding the acquired *D* values (Fig. 8a–c). It is difficult to affirm if the acquired *D* values are significantly different, as the Eyecon® does not allow the presentation of the standard deviation values between the several measurements of a single sample. Nevertheless, assuming that the standard deviation between measurements with this technique is approximately as large as the standard deviations obtained with the other techniques, it is possible to observe a good agreement between the D_{10} and D_{50} values measured for the smaller granule batches b1 and b3 (Fig. 8a and b). Differently, the D_{90} values obtained with Eyecon® are slightly smaller than the ones obtained with Mastersizer® S (Fig. 8c). On the other hand, the granule batch with the largest size, batch b2, had its size overestimated by Eyecon® (Fig. 7b) presenting larger D_{10}, D_{50} and D_{90} values (Fig. 8a–c). These differences of granule size may arise from the fact that, if particles are not conveniently separated, Eyecon® is not capable of individualizing them and provides erroneous results. This demonstrates the importance of a good sampling procedure. Granules need to be efficiently separated to allow the correct identification of the individual particles, hence avoiding errors during the measurement, especially during off-line measurements. During online measurements the distance created between the particles due to their movement should be enough for an accurate detection. In contrast, as pellets are spherical particles with a smooth surface Eyecon® easily can identify the well-defined particle edges successfully individualizing them. The *D* values for the pellet batches (Fig. 8a–c) obtained with Eyecon® and Mastersizer® S revealed a good agreement and are comparable.

3.3. Sieve analysis®

Sieve analysis is a mass-based technique while Mastersizer® S is volume-based. Assuming that all particles have the same density there should not be significant differences between the size data obtained with both techniques. When looking at both size distributions (Fig. 7a–f) and *D* values (Fig. 8a–c) resulting from sieve

analysis, a lack of consistency emerges, especially for pellet batches. As can be observed in the size distributions from pellet batches (Fig. 7d–f) those obtained with the Mastersizer® S are broader than those resulting from sieve analysis and, therefore, larger D_{10} and smaller D_{90} values were expected for sieve analysis in comparison with Mastersizer® S, but this was not the case (Fig. 8a and c). Commonly, D values are estimated from sieve analysis mass percentage distributions by linear regression. This method is not the most adequate as these distributions do not present a linear profile. Given this, it may become difficult to obtain reliable estimates of D values located in the left (D_{10}) or right (D_{90}) ends of the distribution curve. This is also why, from the three interpolated D values, D_{50} values appear to be the most reliable and, therefore, the only one that will be discussed. In comparison with the results provided by Mastersizer® S, the size distributions of granule batches b1 and b3 obtained with sieve analysis shift toward smaller sizes (Fig. 7a and c) and, in accordance, the obtained D_{50} values are also smaller (Fig. 8b). We believe that this might be a result of the erosion of granules during the analysis, even though gentle conditions were used to prevent granule breakage. Sieve analysis is not a method fit for fragile particles as the friction generated during the analysis may deteriorate the sample. Batch b2 was not as similarly affected by erosion and thus the shift toward the left end of the distribution is less evident than for the other granule batches (Fig. 7b) and, also the obtained D_{50} value is not significantly different (Fig. 8b). On the distributions obtained for pellet batches, no shift is perceived when comparing the distributions (Fig. 7d–f) though D_{50} differ slightly (Fig. 8b).

4. Conclusions

In this work, several in-process particle sizing methods and two of the most commonly used off-line methods (sieve analysis and laser diffraction) were reviewed and compared. At first, the differences between all methods were explored theoretically and a table was made in order to facilitate the comparison between the different assessed methods. Further on, the particle size of three batches of granules and three different types of pellets was measured. The laser diffraction Mastersizer® S (wet dispersion method) was utilized as the reference technique. Significant dissimilarities in the measured particle size were observed when comparing all the assayed techniques with the reference method. These differences were elucidated taking into account previous knowledge about the assessed instruments and aimed to simplify the not forthright task of comparing particle size information from different equipments, exposing the reasons for the observed differences rather than finding a correlation between obtained results. The two types of particles that were tested were either homogenous and nearly perfectly spherical (pellets) or porous, almost perfectly spherical aggregates (obtained via a wet granulation method). The effect of particle shape on the estimation of particle size distribution is also of great interest and should be focus of attention if the future.

References

[1] FDA, Guidance for Industry PAT – A Frameword for Innovative Pharmaceutical Development, Manufacturing and Quality Assurance, Process Analytical Technology Initiative, 2004.
[2] A. Burggraeve, T. Van Den Kerkhof, M. Hellings, J.P. Remon, C. Vervaet, T. De Beer, Evaluation of in-line spatial filter velocimetry as PAT monitoring tool for particle growth during fluid bed granulation, Eur. J. Pharm. Biopharm. 76 (2010) 138–146.
[3] A. Burggraeve, T. Van den Kerkhof, M. Hellings, J.P. Remon, C. Vervaet, T. De Beer, Batch statistical process control of a fluid bed granulation process using in-line spatial filter velocimetry and product temperature measurements, Eur. J. Pharm. Sci. 42 (2011) 584–592.
[4] T. Narvanen, Particle size determination during fluid bed granulation – challenges and opportunities, Eur. J. Pharm. Sci. 34 (2008) S12.
[5] I. Masic, I. Ilic, R. Dreu, S. Ibric, J. Parojcic, Z. Duric, An investigation into the effect of formulation variables and process parameters on characteristics of granules obtained by in situ fluidized hot melt granulation, Int. J. Pharm. 423 (2012) 202–212.
[6] A. Burggraeve, N. Sandler, J. Heinamaki, H. Raikkonen, J.P. Remon, C. Vervaet, T. De Beer, J. Yliruusi, Real-time image-based investigation of spheronization and drying phenomena using different pellet formulations, Eur. J. Pharm. Sci. 44 (2011) 635–642.
[7] A. Ali, N. Denis, A.R. Jose, Investigation of on-line optical particle characterization in reaction and cooling crystallization systems. Current state of the art, Meas. Sci. Technol. 13 (2002) 349.
[8] Z.Q. Yu, R.B.H. Tan, P.S. Chow, Effects of operating conditions on agglomeration and habit of paracetamol crystals in anti-solvent crystallization, J. Cryst. Growth 279 (2005) 477–488.
[9] R.D. Braatz, Advanced control of crystallization processes, Annu. Rev. Cont. 26 (2002) 87–99.
[10] A. Rawle, Basic Principles of Particle Size Analysis, Malvern Instruments Ltd., Technical Paper, Worcestershire, UK, 1993.
[11] Z. Ma, H.G. Merkus, J.G.A.E. de Smet, C. Heffels, B. Scarlett, New developments in particle characterization by laser diffraction: size and shape, Powder Technol. 111 (2000) 66–78.
[12] R.M. Jones, Particle size analysis by laser diffraction: ISO 13320, standard operating procedures, and Mie theory, Am. Lab. 35 (2003) 44–47. 44–+.
[13] Mie Theory: The first 100 years, in: Inform, Malvern, 2010.
[14] Particle-size distribution estimation by analytical sieving, Pharm. Eur. 6 (2009).
[15] H. Heywood, Evaluation of powders, J. Pharm. Pharmacol. 15 (1963) 56T–74T.
[16] M.Z. Li, D. Wilkinson, K. Patchigolla, Determination of non-spherical particle size distribution from chord length measurements. Part 2: Experimental validation, Chem. Eng. Sci. 60 (2005) 4992–5003.
[17] D. Petrak, Simultaneous measurement of particle size and particle velocity by the spatial filtering technique, Part. Part. Syst. Charact. 19 (2002) 391–400.
[18] D. Petrak, H. Rauh, Optical probe for the in-line determination of particle shape, size, and velocity, Part. Sci. Technol. 24 (2006) 381–394.
[19] S. Schmidt-Lehr, H.U. Moritz, K.C. Jurgens, Ontine-control of the particle size during fluid-bed granulation/evaluation of a novel laser probe for a better control of particle size in fluid-bed granulation, Pharm. Ind. 69 (2007). 478–+.
[20] M. Fonteyne, J. Vercruysse, D.C. Díaz, D. Gildemyn, C. Vervaet, J.P. Remon, T.D. Beer, Real-time assessment of critical quality attributes of a continuous granulation process, Pharm. Dev. Technol. 18 (2013) 85–97.
[21] D. Petrak, S. Dietrich, G. Eckardt, M. Köhler, In-line particle sizing for real-time process control by fibre-optical spatial filtering technique (SFT), Adv. Powder Technol. 22 (2011) 203–208.
[22] P. Barrett, B. Glennon, Characterizing the metastable zone width and solubility curve using Lasentec FBRM and PVM, Chem. Eng. Res. Des. 80 (2002) 799–805.
[23] E. Kougoulos, A.G. Jones, K.H. Jennings, M.W. Wood-Kaczmar, Use of focused beam reflectance measurement (FBRM) and process video imaging (PVI) in a modified mixed suspension mixed product removal (MSMPR) cooling crystallizer, J. Cryst. Growth 273 (2005) 529–534.
[24] F. Sistare, L. St. Pierre Berry, C.A. Mojica, Process analytical technology: an investment in process knowledge, Org. Process Res. Dev. 9 (2005) 332–336.
[25] A. Tok, X. Goh, W. Ng, R. Tan, Monitoring granulation rate processes using three PAT tools in a pilot-scale fluidized bed, AAPS PharmSciTech 9 (2008) 1083–1091.
[26] B. O'Sullivan, P. Barrett, G. Hsiao, A. Carr, B. Glennon, In situ monitoring of polymorphic transitions, Org. Process Res. Dev. 7 (2003) 977–982.
[27] E. Kougoulos, A.G. Jones, M.W. Wood-Kaczmar, Modelling particle disruption of an organic fine chemical compound using Lasentec focussed beam reflectance monitoring (FBRM) in agitated suspensions, Powder Technol. 155 (2005) 153–158.
[28] Y. Kim, J.R. Méndez del Río, R.W. Rousseau, Solubility and prediction of the heat of solution of sodium naproxen in aqueous solutions, J. Pharm. Sci. 94 (2005) 1941–1948.
[29] D. Greaves, J. Boxall, J. Mulligan, A. Montesi, J. Creek, E.D. Sloan, C.A. Koh, Measuring the particle size of a known distribution using the focused beam reflectance measurement technique, Chem. Eng. Sci. 63 (2008) 5410–5419.
[30] A. Ruf, J. Worlitschek, M. Mazzotti, Modeling and experimental analysis of PSD measurements through FBRM, Part. Part. Syst. Charact. 17 (2000) 167–179.
[31] P.A. Langston, Comparison of least-squares method and Bayes' theorem for deconvolution of mixture composition, Chem. Eng. Sci. 57 (2002) 2371–2379.
[32] M.J.H. Simmons, P.A. Langston, A.S. Burbidge, Particle and droplet size analysis from chord distributions, Powder Technol. 102 (1999) 75–83.
[33] E.J.W. Wynn, Relationship between particle-size and chord-length distributions in focused beam reflectance measurement: stability of direct inversion and weighting, Powder Technol. 133 (2003) 125–133.
[34] P.A. Langston, A.S. Burbidge, T.F. Jones, M.J.H. Simmons, Particle and droplet size analysis from chord measurements using Bayes' theorem, Powder Technol. 116 (2001) 33–42.
[35] M.Z. Li, D. Wilkinson, Determination of non-spherical particle size distribution from chord length measurements. Part 1: Theoretical analysis, Chem. Eng. Sci. 60 (2005) 3251–3265.

[36] W. Liu, N.N. Clark, Relationships between distributions of chord lengths and distributions of bubble sizes including their statistical parameters, Int. J. Multiphase Flow 21 (1995) 1073–1089.
[37] W.D. Liu, N.N. Clark, A.I. Karamavruc, Relationship between bubble size distributions and chord-length distribution in heterogeneously bubbling systems, Chem. Eng. Sci. 53 (1998) 1267–1276.
[38] A. Tadayyon, S. Rohani, Determination of particle size distribution by Par-Tec (R) 100: modeling and experimental results, Part. Part. Syst. Charact. 15 (1998) 127–135.
[39] P.A. Langston, T.F. Jones, Non-spherical 2-dimensional particle size analysis from chord measurements using Bayes' theorem, Part. Part. Syst. Charact. 18 (2001) 12–21.
[40] H.H.J. Bloemen, M.G.M. De Kroon, Transformation of chord length distributions into particle size distributions using least squares techniques, Part. Sci. Technol. 23 (2005) 377–386.
[41] N. Sandler, Photometric imaging in particle size measurement and surface visualization, Int. J. Pharm. 417 (2011) 227–234.
[42] I. Soppela, S. Airaksinen, J. Hatara, H. Raikkonen, O. Antikainen, J. Yliruusi, N. Sandler, Rapid particle size measurement using 3D surface imaging, AAPS PharmSciTech 12 (2011) 476–484.
[43] B. O'Sullivan, Introduction to FBRM technology, Mettler Toledo.
[44] A.R. Heath, P.D. Fawell, P.A. Bahri, J.D. Swift, Estimating average particle size by focused beam reflectance measurement (FBRM), Part. Part. Syst. Charact. 19 (2002) 84–95.
[45] United States Pharmacopeia and National Formulary (USP 28-NF), United States Pharmacopeial Convention, Rockville, MD, USA, 2007.
[46] M. Fonteyne, S. Soares, Y. Vercruysse, E. Peeters, A. Burggraeve, C. Vervaet, J.P. Remon, N. Sandler, T. De Beer, Prediction of quality attributes of continuously produced granules using complementary PAT tools, Eur. J. Pharm. Biopharm (2012).
[47] G. Crawley, Particle sizing online, Powder Metall. 44 (2001) 304–306.
[48] G. Crawley, A. Malcolmson, Online particle sizing as a route to process optimization, Chem. Eng. (N.Y.) 111 (2004) 37–41.